Journal of Energy Challenges and Mechanics
http://www.nscj.co.uk/JECM/

ISSN 2056-9386
Volume 5 (2018) issue 1, article 2

Rheological behaviour and runout of short-lived, fast-moving flows of hot dense suspensions

短暂，快速移动热致密悬浮液的流变行为与流出

Laurence Girolami[1*], Frédéric Risso[2]

[1]*Laboratoire GéHCO, Faculté des Sciences et Techniques, Université de Tours, Campus Grandmont, 37200 Tours, FRANCE*
[2]*Institut de Mécanique des Fluides de Toulouse (IMFT), Université de Toulouse, CNRS, 31400 Toulouse, FRANCE*

laurence.girolami@univ-tours.fr

Accepted for publication on 22th July 2018

Abstract– This study aims at extending the previous work of *Girolami et al.* [11–13] which is still suffering from a lack of reliable predictions for the description of hot, dense suspensions obtained by fluidizing with air a bed of fine solid particles, originally cohesive at room temperature, then released down a rectangular flume. Here, we first present the effective viscosities of the suspensions which increase as a power law of the particle volume fraction Φ_s. Thus, we show that their rheological behaviour is solely controlled by Φ_s and its value at packing $\Phi_{packing}$, whatever the material involved in the mixture. Finally, we present a new modeling of the flows runout and highlight that the flows duration is solely controlled by the settling time (*i.e.* the time necessary for a suspension of a given Φ_s to settle at a velocity U_{sed} over a distance h_{exp} equals to the expansion height), the initial suspension geometry a, and the key parameter $\Phi_s/\Phi_{packing}$. This prediction allows to distinguish two different flow regimes, with a transition around $\Phi_s/\Phi_{packing} \simeq 0.85$, which seems to be correlated to the variations of the mixture rheology.

Keywords– Dense suspensions, rheological behaviour, particle sedimentation, high temperature, runout prediction, scaling laws.

I. INTRODUCTION

Pyroclastic density currents are non-uniform mixtures of hot volcanic ash and gas generated by explosive volcanic eruptions, the most frequently by the gravitational collapse of a lava-dome or the fallback of a Plinian column [1–3]. They are highly mobile, since they can travel large distances (tens of kilometers) around the volcano, as well on the ground as over the sea, at speeds of up to several tens of meters per second. They represent one of the most important hazards around active volcanoes, such as some famous examples of past eruptions [*Montagne Pelée*, Martinique (1902), *Mount Vesuvius*, Italy (AD 79); *Mount Pinatubo*, Philippines (1991); *Mount Unzen*, Japan (1990-1995)], which entirely destroyed the proximal areas located around the volcano, have caused the death of up to 30,000 people, whilst their destructive effects have continued for many decades after the disaster itself [4–6].

One particular aspect of these flows, that plays an important role in controlling their dynamics, is their ability to become rapidly and strongly vertically stratified [1; 2; 7], such as forming two approximate end members: (1) a thin concentrated underflow, *named a pyroclastic flow*, which commonly fills the valleys due to its high bulk density and whose mobility is drastically enhanced by the fluidization effects; (2) an upper dilute surge, whose mobility is principally attributed to the mixture turbulence, thus passing over topographic barriers (of up to thousands-meters-height) such as easily de-coupling from its dense underflow, which tends to remain guided by topography and to be more predictable.

The fluidization processes, that are largely developed in basal pyroclastic flows [7–9], act in significantly reducing the friction between particles, thus increasing the flows mobility and more specifically their ability to travel a large distance down gentle slopes, with degrees quite inferior to that determined by the internal friction angle of the hot material involved in the mixture [10]. The present study focuses on the behaviour of such basal pyroclastic flows, which control the transport and the sedimentation of the quasi-totality of the mixture's mass. They form massive deposits, *termed ignimbrites*, from which it is however difficult to infer the original flow dynamics. Therefore, it is important to access to these complex processes in the laboratory in order to better infer the flow dynamics from the deposits morphology.

In this way, *Girolami* [10] succeeded in reproducing experimentally such rapid sheared flows made of hot, dense suspensions, using a laboratory lock-exchange flume capable of withstanding to high temperatures. The material (volcanic ash and chemical catalysts) was initially fluidized in a locked reservoir, thus uniformly expanded (up to 50 vol% above loose packing), whilst heated at 200°C to discard from the cohesive effects associated with atmospheric moisture. Once expanded at a given value, the fluidized suspension characterized by a well constrained geometry, was released down a smooth, horizontal, and impermeable flume such as defluidizing progressively until it ran out of mass [11].

In these previous studies [11–13], the authors especially investigated the effect of the dilatation rate of the bed (termed *initial expansion*) on the flow kinematics, the velocity fields, the internal flow structures, as well as the deposits morphologies [11–13], using high-speed videos, which were subsequently analyzed in aid of a particle-tracking algorithm (*see* [12]). In all experiments, the flows were highly sheared, such as exhibiting a slightly concave-upward velocity profile. The maximum internal velocity was closed to that of the flow front, while decreasing slightly towards the free surface, possibly due to the air drag. The particles settling was observed to start just after the gravitational slumping, by forming a loose deposit which progressively thickened from the base, as observed in both dry [14–15] and aerated granular flows [16], such as considering a basal no-slip condition at the back of the frontal region. The aggradation rates of particles, measured from the expanded flows, highlighted that the sedimentation processes were delayed when the fluidizing gas velocity was increased as well as the initial bed expansion E. However, the sedimentation rates remained approximately constant with time in the proximal regions of the flows (for a given E) and with most of the runout duration, while they strongly increased during their last, decelerating phase of emplacement. One of their major findings highlighted that the deposit aggraded at a mean velocity identical to that inferred to take place at the base of a non-sheared collapsing bed (*i.e.* with the lock gate closed) at a given value of E. However, no universal scaling laws able to describe and predict the flows behaviour have been provided. Therefore, some complementary studies are required to provide a physical description of these flows, including their rheological features, which still fail in large-scale numerical simulations. This step also represents the starting point for the development of probabilistic hazard mapping required for the risks assessment and mitigation, which is the priority of modern volcanology. Such tools may help the local authority to take some crucial decisions in case of evacuation during a crisis period.

This present study aims at revisiting the past investigations of *Girolami et al.* [11–13] by extending their results and discussions which are still suffering from a lack of a deep understanding and prediction of such complex systems. In this way, we present here a new analysis of these flows based on previous experimental data [11–13] and propose original findings that will improve their physical description. This study should have an important impact on the understanding of hot dense, suspensions of gas-solid mixtures and their natural behaviour, such as the emplacement of small volume pyroclastic flows (*i.e.* block-and-ash flows), commonly generated by the partial collapse of a lava-dome or an entirely collapsing pyroclastic fountain.

II. Fluidization Concepts

2.1. Behaviour of hot, dense fluidized suspension

The fluidization processes that are largely developed in dense pyroclastic flows can be reproduced in the laboratory by injecting uniformly a vertical gas stream (passing through a porous plate) at the base of a static bed of particles. Then, we can observe different regimes of fluidization which depend on the fluidizing gas velocity [17–18].

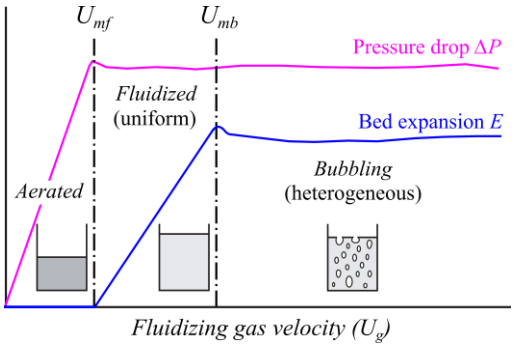

Fig.1 Pressure drop ΔP across the bed thickness h and mixture expansion E defined as the height ratio between the expanded mixture and the packed bed) as a function of the fluidizing gas velocity for fine, non cohesive powders [17–18].

When the gas flow is weak, the fluid passes through interstitial voids without modifying the state of the bed, such as the bed is termed *aerated*. In this state, the bed expansion rate E remains static (see the *blue curve* on Fig. 1) whilst the gas pressure drop across the bed ΔP (see the *pink curve* on Fig. 1) increases linearly with the fluidizing gas velocity since the friction exerted by particles is dominated by viscous stresses which are proportional to the gas flow, as described by the semi-empirical equation of *Ergun* (1952) [19]:

$$\frac{\Delta P}{h} = \frac{150\mu_g\,(1-\epsilon)^2\,U_g}{\epsilon^3 {d_p}^2} + \frac{1.75\rho_g\,(1-\epsilon)\,{U_g}^2}{\epsilon^3 d_p} \qquad (1)$$

where ΔP represents the gas pressure across the bed thickness h, ϵ the bed voidage, μ_g: the gas dynamic viscosity at 200°C, U_g: the superficial gas velocity (defined as the gas flow rate normalized by the cross sectional area), d_p: the particle diameter, and ρ_g: the gas density.

If the gas stream is increased further, the *velocity of minimum fluidization* is reached. At this point, the driving forces counterbalance the gravitational ones and the total weight of particles is entirely supported by the gas flow, such as:

$$\frac{\Delta P}{h} = g\,(1-\epsilon_{mf})\,\rho_p \qquad (2)$$

where ϵ_{mf} represents the voidage at the point of *minimum fluidization* U_{mf}, ρ_p: the particles density, ρ_g: the gas density, and

g: the gravitational acceleration. In this state, the mixture forms a dense suspension whose mobility is greatly increased and which may be easily sheared and superficially behaves as a fluid [20]. If particles are fine enough (*i.e.* Group A in the *Geldart Classification* [21]), the mixture expands uniformly with the increasing gas velocity such as the bed height increases linearly whilst the pressure gradient becomes independant of the gas flow (Fig. 1).

This state is observed until a second critical velocity (*the velocity of minimum bubbling*, U_{mb}) above which bubbles form at the surface of the distributor plate and coalesce as they rise, thus disturbing the fluidization and making it unstable, with a vigorous mixing and turbulence. Bubbles are however rapidly broken by turbulence such as maintaining the bed expansion approximately constant and closed to its maximum value. Above this point, the bed height as well as the pressure gradient across the bed are independent of the gas stream (Fig. 1).

However, these different regimes of fluidization depend on the type of material used and on the conditions of operation. For example, with coarse and/ or dense materials, the uniform (particulate) regime of fluidization (developed between U_{mf} and U_{mb} with fine powders) is not observed and the bubbling regime directly follows the aerated state. Otherwise, when the material is fine and originally highly cohesive, the fluidization is impeded since the gas solely flows through channels across the most permeable regions of the bed such as the bed weight can not be fully supported and the bed expansion remains quasi-inexistent. The fluidization of fine materials can be thus improved by both heating as well the powders as the fluidizing gas, at temperatures high enough (closed to 150° C), to avoid the strong cohesive effects of moisture; and by stirring vigorously the bed to prevent the gas channeling. In this way, the fluidization of fine, cohesive (termed as *Group C powders* in the *Geldart Classification* [21]) is henceforth possible and characterized by a uniform volume expansion (up to few tens vol%) above loose packing.

2.2. Bed Collapse Test

If we cut abruptly the gas supply, the bed will defluidize progressively by expelling the interstitial gas, then forming a loose deposit that will aggrade progressively from the base.

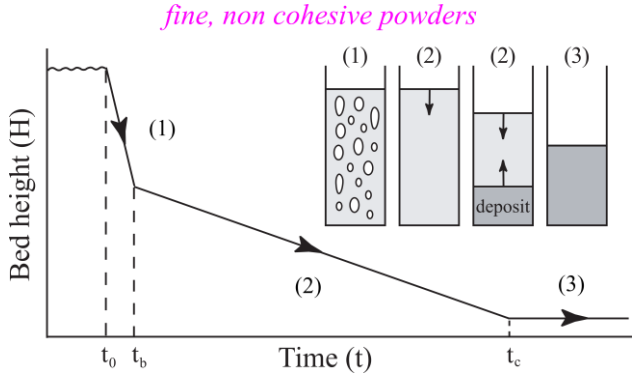

Fig.2- Gas escape and sedimentation of the bed surface during a collapse test that has been performed after having rapidly turned off the gas supply for Group-A (fine, non cohesive) powders of the *Geldart Classification* [21]. t_0 represents the initial time at which the gas supply was abruptly turned off, t_b represents the time of bubbles expulsion, t_c represents that associated with a uniform defluidization (or compaction) that ultimately forms a loosely packed bed [25].

This process is termed a *bed collapse-test* and allows to measure easily the sedimentation velocity of the bed surface [22–25]. In this study, we focus on the uniform fluidization regime obtained between U_{mf} and U_{mb}, in order to gain quantitative measurements of both expansion and sedimentation velocities (Fig. 2).

III. Experimental Methods

3.1. Materials Properties

One of the principal objectives of this study was to compare the expansion and sedimentation behaviour of volcanic ash with synthetic materials. Samples of natural material, involved in the experiments, were collected from an ignimbritic deposit (located at Neshers, in the French Massif Central); thus sieved to keep only the fine fraction (*i.e.* inferior to 250μm). This material was characterized by a weak permeability (*i.e.* of the order of 10^{-11} m^{-2}, *see* Table 2), a porous texture, and a strong irregular shape (Fig. 3). Two natural samples (*Ash*[1], *Ash*[2]) were investigated, both exposing a high poly-dispersity.

Size range (μm)	*250-180*	*180-125*	*125-90*	*90-63*	*63-45 < 63*	*45-32*	*32-0*
Ash[1] (wt %)	8.44	12.36	14.26	18.67	46.27		
Ash[2] (wt %)	6.09	10.51	10.41	12.72	60.27		
FCC (wt %)	0.05	2.01	15.35	39.95	26.36	11.27	5.01

Tab.1- Granulometric distribution of the particles involved in the experiments. *Ash*[1] and *Ash*[2] represent the data obtained with ash: *sample 1* and *sample 2* respectively.

Sample 1 has a coarser granulometric distribution (*see Ash*[1] in Table 1), with a mean particle diameter $d_p \simeq 79.7\mu$m. *Sample 2* is enriched in fine ash, with a mean particle diameter $d_p \simeq 64.7\mu$m (*see Ash*[2] in Table 1). In order to compare their physical behaviour with a more simple material, experiments also involved synthetic chemical catalysts (named *FCC*) commonly used in the oil industry. These powders have a more regular shape (Fig. 3) with a similar mean particle diameter ($d_p \simeq 71\mu$m) which highlights their slightly cohesive nature at room temperature (*i.e.* from Group C to Group A in the *Geldart Classification* [21]).

3.2. Key Parameters

When the bed is aerated, the superficial gas velocity U_g, passing through the interstitial voids, is given by the Darcy's Law, such as:

$$U_g = \frac{K}{\mu_g}\left(\frac{\Delta P}{h} + \rho_g g\right) \quad (3)$$

where K is the bed permeability, μ_g: the viscosity of the hot gas, such as: $\mu_g = 2.45\times10^{-5}$ Pa.s, ΔP represents the gas pressure drop across the bed thickness h measured with a differential pressure sensor placed at the back of the fluidization rig, ρ_g: the density of the hot gas, such as: ρ_g =

0.79 kg.m^{-3} and g: the gravitational acceleration. At the point of *minimum fluidization*, we can determine the bed permeability, such as:

$$K_{mf} = \mu_g \frac{U_{mf}}{\left(\frac{\Delta P}{h} + \rho_g g\right)} \quad (4)$$

where U_{mf} is the superficial gas velocity at the point of *minimum fluidization.* The bed porosity ϵ_{mf} was deduced from *Eq*. (2) (taking ρ_g= 0.79 kg.m^{-3}, and measurements of ρ_p, see Table 2, performed with a pycnometer). The key physical parameters, that characterize the different powders used in the experiments, are summarized on Table 2.

Key Parameters	*Ash* [1]	*Ash* [2]	*FCC**
U_{mf} (m.s^{-1})	0.0028	0.0019	0.0031
U_{mb} (m.s^{-1})	0.0087	0.0068	0.0089
Particle density ρ_p $(kg.m^{-3})$	1600	1490	1420
Mean diameter d_p (μm)	79.7	64.7	71
Bed permeability K_{mf} (m^{-2})	1.06 10^{-11}	7.7 10^{-12}	
Packing porosity ϵ_{mf}	0.42	0.4	0.51

Tab.2- Physical parameters determined for the different materials used in this study. *Ash*[1] and *Ash*[2] represent the key parameters obtained with ash: *sample 1* and *sample 2* respectively. *FCC* represents the parameters obtained for the *FCC-catalysts* and completed with [26]. The density and viscosity of the hot fluidizing gas injected are respectively: ρ_g = 0.79 kg.m^{-3} and μ_g = 2.45×10^{-5} Pa.s.

3.3. Experimental Procedures

Experiments were carried out in a linear lock-exchange flume capable of withstanding to high temperatures (Fig. 3). The interest of such dam-break configurations is the ability to properly control the parameters related to the initial geometry of the mixture (*i.e.* its initial expanded height h_0, its length x_0, its width w_0, its initial dilatation rate E). The operating temperature (180°C) was justified by previous results gained from 1-D collapse-tests of volcanic ash [25] which highlighted that their fluidization behaviour was similar, to a first order, at temperatures ranged from 200°C to 700°C, provided that the cohesive effects are negligible. So, it was sufficient to work at temperature closed to 200°C to approach the natural conditions in which ignimbritic deposits are resulting from the hindered settling of pyroclastic flows.

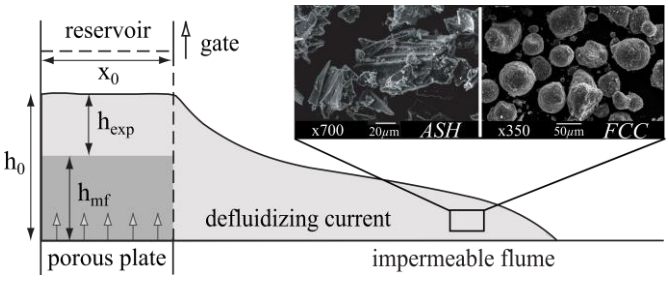

Fig.3- Scheme of the rectangular dam-break flume which allows to well constrain initially the operating parameters studied in the experiments.

The role of the operating parameters were principally explored: (1) the initial aspect ratio a which was defined as the ratio between the height h_0 of the fluidized suspension before release and its length x_0 in the reservoir and ranged from 0.5 to 4; (2) the mixture dilatation rate E, which was defined as the ratio between h_0 and h_{mf}: the height of the packed bed (see Fig. 3), ranged from 1.0 to 1.5. In the present study, two sets of experiments were repeated with different materials (Ash: *sample 1* & *sample 2*, *FCC-catalysts*) and analyzed. The first series of experiments was performed at a constant volume (*i.e.* with a similar column geometry: a = 0.5), whilst the mixture dilatation rate was increased by decreasing the initial mass poured in the reservoir (*i.e.* decreasing the initial packed height h_{mf}, such as E = 1.0–1.5). The second series of experiments was performed at constant mass (*i.e.* introducing a constant h_{mf}) whilst the mixture dilatation rate was increased by increasing the initial volume (a = 0.5–0.85; E = 1.0–1.5).

The experimental procedures consisted in first pouring the hot material in the reservoir, thus injecting a hot gas flow, uniformly at the base of the bed. Once the given expansion was reached and the gas supply was turned off, the sliding gate was opened in order to release the suspension that defluidized progressively down the smooth, horizontal channel, until motion ceased (Fig. 3).

IV. Suspension Behaviour

4.1. Particles Sedimentation

The sedimentation velocities of the bed surface, which corresponds to the gas escape velocities (termed *hindered settling velocities*), were first measured from the bed collapse-tests performed in the reservoir at both different fluidization and dilatation rates. Measurements of *hindered settling velocities* (reported in *white* on Fig. 4) are observed to decrease linearly with increasing particles volume fractions Φ_s= 1- ϵ. The data were directly compared with the superficial gas velocities (reported in *dark grey* on Fig. 4) and exposed similar values. Thus, the velocity at which the bed settles once the gas supply is turned off is similar to that necessary to expand the bed at a given voidage.

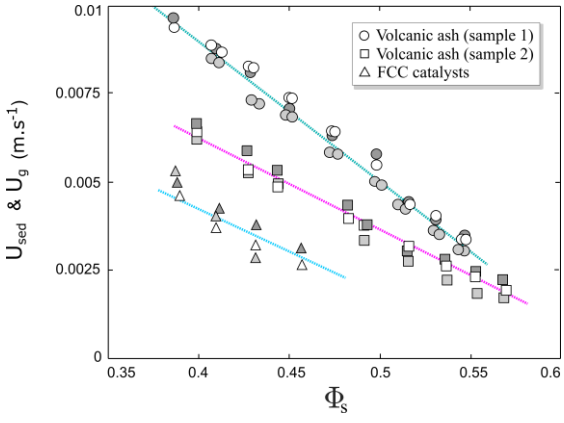

Fig.4- Hindered settling velocities U_{sed} (measured from both the non-sheared bed collapse test and represented by *white* symbols as well as from defluidizing flows and represented by l*ight grey* symbols) and superficial gas velocities U_g (represented by *dark grey* symbols) as a function of the particle volume fraction Φ_s.

Moreover, the sedimentation velocities measured from proximal flows, at the vicinity of the sliding gate, after having released the mixture down the flume (*i.e.* from similar suspensions than those resulting from the static bed collapse-tests) are thus reported in *light grey* on Fig. 4. These values are similar to those measured from non-sheared bed collapse tests at a given Φ_s and show that particles sedimentation velocities in proximal flows can be predicted from the initial parameter U_g.

4.2. Mixtures viscosities

The velocity U_0 of a single spherical particle characterized by its diameter d_p falling in a fluid of viscosity μ_g and of density ρ_g is given by the *Stokes velocity*, such as:

$$U_0 = \frac{g\,(\rho_p - \rho_g)\,{d_p}^2}{18\mu_g} \tag{5}$$

This velocity is reliable for dilute suspensions in which the settling processes are not disturbed by the global motion of the neighbouring particles. However, *Richardson & Zaki* [27] have rewritten this terminal velocity for the dense case by considering a particle falling in a mixture of density ρ_m and viscosity μ_m, such as:

$$U_{sed} = \frac{g\,(\rho_p - \rho_m)\,{d_p}^2}{18\mu_m} \tag{6}$$

From Eq. 6, we can determined the effective viscosity of the mixture, such as:

$$\mu_m = \frac{g\,(\rho_p - \rho_m)\,{d_p}^2}{18U_{sed}} \tag{7}$$

where ρ_m is the mixture density that can be recalculated for each value of ϵ and Φ_s, such as:

$$\rho_m = (1 - \phi_s)\rho_g + \phi_s\rho_p \tag{8}$$

Note that ϵ and Φ_s were determined from values of ϵ_{mf} and E.

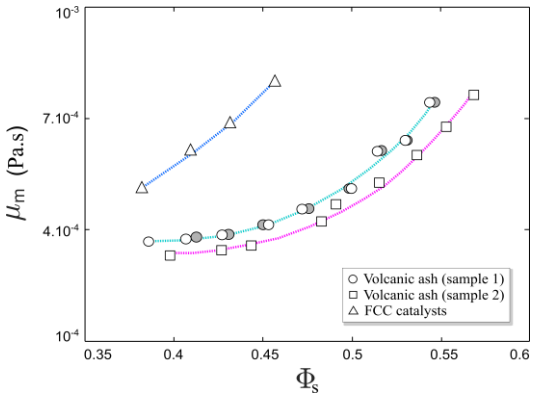

Fig.5- Effective viscosities of fluidized suspensions μ_m calculated from Eqs. (7) – (8) as a function of the particle volume fraction Φ_s.

As exposed on Fig. 5, the mixture viscosity μ_m increases with increasing particles volume fraction Φ_s, while following different laws which depend on the materials properties (*see* Table 2).

4.3. Rheological law

By plotting the effective mixture viscosities μ_m normalized by the hot fluidizing gas viscosity μ_g as a function of the particle volume fraction Φ_s normalized by its value at packing $\Phi_{packing}$, we observe that all the experimental data collapse such as following a main trend which represents the rheological behaviour of such hot, dense suspensions made of different materials (Fig. 6).

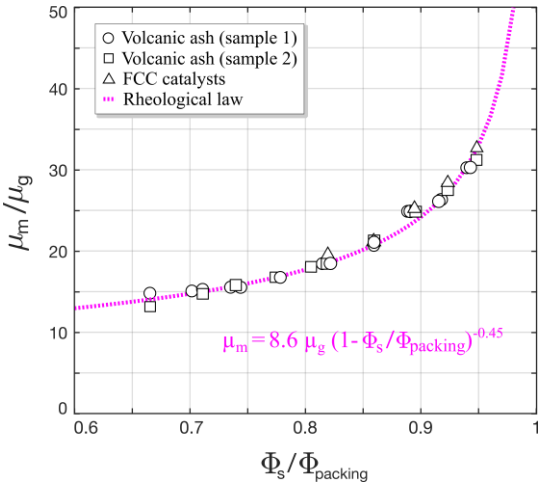

Fig.6- Rheological law obtained for the hot fluidized suspensions.

This rheological law is thus identical for both two distinct samples of highly polydisperse and porous volcanic ash and one sample of well sorted, roughly spherical synthetical powders (Fig. 6). This description is expressed as follows:

$$\mu_m = 8.6\mu_g\left(1 - \frac{\phi_s}{\phi_{packing}}\right)^{-0.45} \tag{9}$$

Eq. (9) highlights that the rheological behaviour of such suspensions only depends on the particles volume fraction and its value at packing. This law remains however relevant for the dense regime (closed to the packing state) but can not be valid anymore in the dilute regime.

Thus, for low values of $\Phi_s/\Phi_{packing}$, (*i.e.* when $\Phi_s/\Phi_{packing} \rightarrow 0$), the viscosity remains 8.6 times higher than that of the hot gas. On the other hand, for high values of $\Phi_s/\Phi_{packing}$ (*i.e.* when $\Phi_s/\Phi_{packing} \rightarrow 1$), the viscosity drastically increases and tends to infinity around the packing state, as expected.

V. Runout Prediction

One of the principal objectives of this study, guided by geophysical interests, was also to provide scaling laws able to describe both the runout duration and the runout length as a function of the key parameter $\Phi_s/\Phi_{packing}$ which controls the mixture rheology.

Fig. 7 exposes the flow duration t_∞ normalized by the time t_{sed} required for a suspension of a given Φ_s to settle at a velocity U_{sed} (measured from static bed collapse-tests) over a distance h_{exp} (which corresponds to the gas height initially controlled by the dilatation rate, *see* Fig. 3), corrected by a geometric factor $a^{-1/2}$ (where a is the aspect ratio of the suspension in the reservoir), as a function of the key non-dimensional parameter $\Phi_s/\Phi_{packing}$.

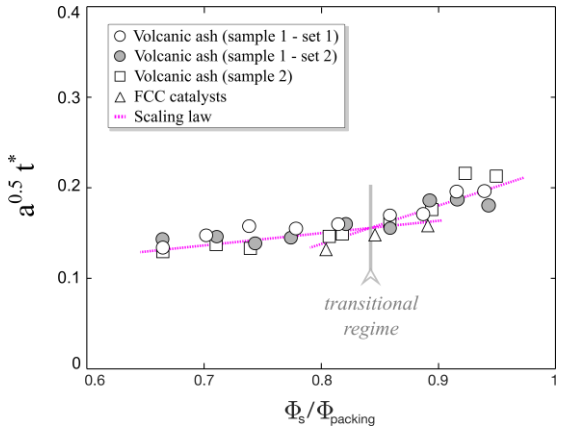

Fig.7- Flows duration normalized by the settling time as a function of the key parameter $\Phi_s/\Phi_{packing}$.

All experimental data performed with the different materials are observed to collapse into a single master curve which indicates that the flow duration t_∞ is indeed controlled by the mixture sedimentation velocity, the initial aspect ratio of the suspension and the mixture rheology, such as:

$$t_\infty \propto a^{-1/2} \left(\frac{h_{exp}}{U_{sed}}\right) \left(\frac{\phi_s}{\phi_{packing}}\right) \tag{10}$$

We can however distinguish two different trends: (1) for $0.65 < \Phi_s/\Phi_{packing} < 0.85$ which corresponds to the most weakly concentrated, highly expanded flows; and (2) for $\Phi_s/\Phi_{packing} \geq 0.85$ which corresponds to the most highly concentrated, weakly expanded flows with a transition around $\Phi_s/\Phi_{packing} \simeq 0.85$, represented in *grey* on Fig. 7.

Using the mean flow velocity U_{moy} (simply determined as the ratio between the final distance traveled by the flow and its duration), we can similarly plot the non-dimensional ratio between the runout distance x_∞ and that required for a suspension of a given Φ_s to settle at a velocity U_{sed} over a distance h_{exp}, including the geometric correction factor $a^{-1/2}$ as a function of the key parameter $\Phi_s/\Phi_{packing}$ (Fig. 8).

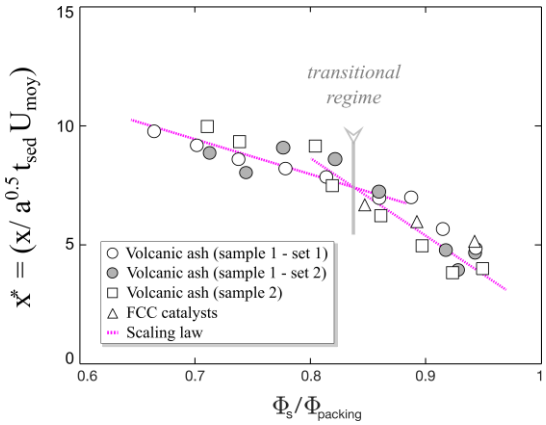

Fig.8- The final traveled distance normalized by the settling length as a function of the key parameter $\Phi_s/\Phi_{packing}$.

Similarly, all experimental data involving the different materials, collapse into a single master curve which indicates that the runout distance x_∞ is also controlled by the sedimentation processes, the initial geometry of the suspension as well as the mixture rheology, such as:

$$x_\infty \propto a^{-1/2} \left(t_{sed} \cdot U_{moy}\right) \left(\frac{\phi_s}{\phi_{packing}}\right) \tag{11}$$

We can also distinguish two similar trends: (1) for $0.65 < \Phi_s/\Phi_{packing} < 0.85$; and (2) for $\Phi_s/\Phi_{packing} \geq 0.85$ with a transition around $\Phi_s/\Phi_{packing} \simeq 0.85$, represented in *grey* on Fig. 8.

This transition may indicate that runouts would probably depend on the mixture rheology.

VI. Concluding Remarks

This study presents new insights gained from a recent analysis of previous experimental data [11–13] that have been revisited following geophysical interests which consist in better understanding the rheological behaviour and the emplacement mechanism of dense pyroclastic flows resulting from explosive volcanic eruptions. Hence, the major findings concern:

(1) The rheological behaviour of hot, dense suspensions which is solely controlled by the particle volume fraction and its value at packing, whatever the material used. This empirical law turns out to be reliable for dense suspensions only (*i.e.* for $0.38 < \Phi_s < 0.58$) and should not be extrapolated to dilute cases.

(2) The predictions of the flows duration (*i.e.* once the suspension was released down the dam-break flume) is controlled by the settling time (*i.e.* the time necessary for a suspension of a given Φ_s to settle at a velocity U_{sed}, measured from static bed-collapse-tests, over a distance h_{exp} equals to the gas height), the initial geometry $a^{-1/2}$, and the particle volume fraction normalized by its value at packing $\Phi_s/\Phi_{packing}$ (which amounts at considering the material properties). This prediction allows to distinguish two different flow regimes, with a transition around $\Phi_s/\Phi_{packing} \simeq 0.85$, which seems to be correlated to the sharp variation of the mixture rheology.

REFERENCES

[1] R.V. Fisher and H.U. Schmincke, *Submarine volcaniclastic rocks.* In: Pyroclastic Rocks, Springer Berlin: Heidelberg. 1984.

[2] R.A.F. Cas and J.V. Wright, *Volcanic successions: modern and ancient*, London: Allen and Unwin, 1987.

[3] P. Francis, C. Oppenheimer, and D. Stevenson, "Endogeneous growth of persistently active volcanoes*", Nature*, **366**, pp. 554-557, 1993.

[4] M.R. Rampino, and S. Self, "Volcanic winter and accelerated glaciation following the Toba super-eruption*", Nature*, **359**(6390), pp. 50, 1992.

[5] A. Robock, "Volcanic eruption and climate*", Review of Geophysics*, **38**(2), 191-219, 2000.

[6] S. Dartevelle, G.G. Ernst, J. Stix, and A. Bernard, "Origin of the Mount Pinatubo climactic eruption cloud: Implications for volcanic hazards and atmospheric impacts*", Geology*, **30**(7), 663-666, 2002.

[7] T.H. Druitt, "Pyroclastic density currents*", Geological Society: London, Special Publications*, **145**(1), pp. 145-182, 1998.

[8] R.S.J. Sparks, "Grain size variations in ignimbrites and implications for the transport of pyroclastic flows*", Sedimentology*, **23**(2), pp. 147-188, 1976.

[9] C.J.N. Wilson, "The role of fluidization in the emplacement of pyroclastic claws: An experimental approach*", Journal of Volcanology and Geothermal Research*, **8**(2), pp. 231-249, 1980.

[10] L. Girolami, *Dynamique et sédimentation des écoulements pyroclastiques reproduits en laboratoire*, Doctoral dissertation, Clermont-Ferrand-2, 2008.

[11] L. Girolami, T.H. Druitt, O. Roche, and Z. Khrabrykh, "Propagation and hindered settling of laboratory ash flows*", Journal of Geophysical Research: Solid Earth*, **113**(B2), 2008.

[12] L. Girolami, O. Roche, T.H. Druitt, and T. Corpetti, "Particle velocity fields and depositional processes in laboratory ash flows, with implications for the sedimentation of dense pyroclastic flows*", Bulletin of Volcanology*, **72**(6), pp. 747-759, 2010.

[13] L. Girolami, T.H. Druitt, and O. Roche, "Towards a quantitative understanding of pyroclastic flows: effects of expansion on the dynamics of laboratory fluidized granular flows*", Journal of Volcanology and Geothermal Research*, **296**, pp. 31-39, 2015.

[14] A. Wachs, L. Girolami, G. Vinay, and G. Ferrer, "Grains-3D, a flexible DEM approach for particles of arbitrary convex shape—Part I: Numerical model and validations*", Powder Technology*, **224**, pp. 374-389, 2012.

[15] L. Girolami, V. Hergault, G. Vinay, and A. Wachs, "A three-dimensional discrete-grain model for the simulation of dam-break rectangular collapses: comparison between numerical results and experiments*", Granular Matter*, **14**(3), pp. 381-392, 2013.

[16] O. Roche, M.A. Gilbertson, J.C. Phillips, and R.S.J.. Sparks, "Experimental study of gas-fluidized granular flows with implications for pyroclastic flow emplacement*", Journal of Geophysical Research: Solid Earth*, **109**(B1), 2004.

[17] M.J. Rhodes, *Introduction to Particle Technology*, John Wiley: Hoboken, N. J., 1998.

[18] L.S. Fan, and C. Zhu, *Principles of gas-solid flows*, *Cambridge University Press*, pp. 557, N. J., 1998.

[19] S. Ergun, "Fluid Flow through Packed Columns*", Chemical Engineering Progress*, **48**, pp. 89-94, 1952.

[20] I. Eames, and M.A. Gilbertson, "Aerated granular flow over a horizontal rigid surface*", Journal of Fluid Mechanics*, **424**, 169-195, 2000.

[21] D. Geldart, "Types of gas fluidization*", Powder Technology*, **7**, 285-292, 1973.

[22] D. Geldart, and A.C.Y Wong, "Fluidization of powders showing degrees of cohesiveness, II, Experiments on rates of deaeration*", Chemical Engineering Sciences*, **40**, 653-661, 1985.

[23] P. Lettieri, J.G. Yates, and D. Newton, "The influence of inter-particle forces on the fluidization behaviour of some industrial materials at high temperature*", Powder Technology*, **110**, pp. 117-127, 2000.

[24] G. Bruni, P. Lettieri, D. Newton, and J. Yates, "The influence of fines size distribution on the behaviour of gas fluidized beds at high temperature*", Powder Technology*, **163**, pp. 88-97, 2006.

[25] T.H. Druitt, G. Avard, G. Bruni, P. Lettieri, and F. Maez, "Gas retention in fine-grained pyroclastic flow materials at high temperatures*", Bulletin of Volcanology*, **116**(7), pp. 881, 2007.

[26] P. Lettieri, D. Newton, and J.G. Yates "Homogeneous bed expansion of FCC catalysts, influence of temperature on the parameters of the Richardson–Zaki equation*", Powder Technology*, **123**, pp. 221-231, 2002.

[27] J.F. Richardson, and W.N. Zaki "The sedimentation of a suspension of uniform spheres under conditions of viscous flow*", Chemical Engineering Science*, **3(2)**, pp. 65-73, 1954.